SUPPLEMENTARY MATERIAL

Early growth and environmental conditions control partial migration of an estuarine-dependent fish

Kohma Arai[1,2,*], Jessica E. Best[3], Caitlin A. Craig[4], Vyacheslav Lyubchich[1], Nathaniel R. Miller[5], David H. Secor[1]

[1]Chesapeake Biological Laboratory, University of Maryland Center for Environmental Science, Solomons, MD 20688, USA
[2]Center for Watershed Sciences, University of California, Davis, Davis, CA 95616, USA
[3]New York State Department of Environmental Conservation, Division of Marine Resources, Department of Natural Resources, Cornell University, New Paltz, NY 12561, USA
[4]New York State Department of Environmental Conservation, Division of Marine Resources, Kings Park, NY 11754, USA
[5]Jackson School of Geosciences, The University of Texas at Austin, Austin, TX 78712, USA

*Corresponding author: kharai@ucdavis.edu

Text S1. Ageing bias and precision

To evaluate ageing bias and precision, a subsample (n = 30) of juvenile striped bass otoliths was read twice by the same reader. Prior to the exercise, the reader had received training and had previous experience reading daily increments in striped bass otolith microstructure. Systematic bias in matched pairs of ages between the two reads was assessed using paired t-test and the test of symmetry (Hoenig et al. 1995), and was visually assessed through age-bias plots (Campana et al. 1995). Precision between matched pairs was quantified as the mean coefficient of variation (CV) following the method by (Chang 1982).

The average age difference was 1.6 days and was within 4 days for all matched pairs analyzed. Daily increment counts from the two reads closely followed the identity line (i.e., replicate estimated ages are equal) of the age-bias plot (Fig. S2). No systematic bias was detected between the two reads (paired t-test, p = 0.076; test of symmetry, p = 0.293). Ageing precision between the two reads measured in the form of mean CV was 1.5%, indicating very high precision compared to literature values (Campana 2001).

Text S2. Spawning locations inferred from core otolith chemistry

We assessed otolith chemistry near the otolith core region to assess whether distinct migration contingents were associated with different spawning locations. We averaged otolith chemistry (i.e., Mg, Mn, Sr, Ba) measured just outside the core region corresponding to back-calculated total length of 6–8 mm. This region was chosen based on visual assessment of otolith elemental profiles: the region after maternal signatures had mostly disappeared and just before the otolith chemistry exhibited non-natal habitat signatures. We then conducted a principal component analysis on averaged otolith chemistry signatures to assess the presence of multiple spawning locations.

For both 2019 and 2020, assigned migration contingents substantially overlapped in the principal component space with no apparent sub-grouping (Fig. S3). Outliers were represented by early migrants that showed non-natal signatures near the core region. Thus, we found no indication of early migration contingents associated with distinct spawning locations.

Text S3. The effect of hatch dates and early life experiences on larval growth

To assess how hatch dates and early life environmental conditions influence larval growth, we employed a generalized linear model with a gamma distribution and a log link function. Larval growth was modeled as a continuous response variable, and the first principal component score (PC1, strong loadings of hatch dates, and experienced mean temperature, flow, and chlorophyll-a) was included as a continuous predictor. Separate models were fitted to 2019 and 2020 data.

The estimated coefficient of the GLM showed a significant positive relationship between PC1 and larval growth for 2019 (coefficient ± SE = 0.013 ± 0.006, p = 0.024), indicating that faster larval growth was associated with later hatch dates exposed to higher temperature, lower flow, and higher chlorophyll-a concentration. However, the coefficient of the GLM for 2020 showed no significant relationship between PC1 and larval growth (coefficient ± SE = 0.008 ± 0.008, p = 0.331).

Text S4. Univariate comparison of hatch dates and early life experiences

Two-way analysis of variance (ANOVA) with a gamma distribution and a log link was used to test differences in hatch dates and early life experiences (i.e., mean water temperature, river flow, and chlorophyll-a) of age-0 juveniles across migration contingents, years (2019 and 2020), and their interaction. When Levene's test detected unequal variances across the years, the model was fitted using the Generalized Additive Model for Location, Scale, and Shape (GAMLSS) in the R package "*gamlss*" (Rigby & Stasinopoulos 2005), which allowed for different variances per treatment (i.e., heteroscedastic). A post-hoc Tukey test was further employed for multiple comparisons of these variables across contingents within each year using the "*emmeans*" R package (Lenth et al. 2018).

For hatch dates, significant effects of contingent (two-way ANOVA, $F_{3,123} = 5.09$, $p = 0.002$), year ($F_{1,123} = 102.59$, $p < 0.001$), and their interaction ($F_{3,123} = 8.77$, $p < 0.001$) were detected. In 2020, post-hoc contrasts indicated that oligohaline migrants hatched significantly later compared to residents (Tukey test, $p = 0.014$) and large mesohaline migrants ($p < 0.001$), whereas large mesohaline migrants hatched significantly earlier compared to their peers ($p < 0.01$; Fig. S5A). No significant differences in hatch dates were detected across contingents in 2019, although hatch dates on average occurred later in 2019 compared to 2020. Mean temperature exposure during the first 30 days of life was significantly affected by contingent (two-way ANOVA, $F_{3,121} = 7.90$, $p < 0.001$) with a significant interaction effect between year and contingent ($F_{3,121} = 10.94$, $p < 0.001$). As a result of differences in hatch dates in 2020, oligohaline migrants experienced significantly higher temperatures compared to residents (Tukey test, $p = 0.038$) and large mesohaline migrants ($p < 0.001$), whereas large mesohaline migrants were exposed to significantly cooler temperatures compared to their peers ($p < 0.001$; Fig. S5B). No significant differences in experienced temperature were detected across contingents for 2019 given similar hatch dates. Mean river flow experienced during the first 30 days of life was significantly influenced by contingent (two-way ANOVA, $F_{3,121} = 8.20$, $p < 0.001$), year ($F_{1,121} = 3520.71$, $p < 0.001$), and their interaction ($F_{3,121} = 10.80$, $p < 0.001$). Post-hoc contrasts showed that large mesohaline migrants experienced significantly higher flow compared to their counterparts in 2020 given earlier hatch dates (Tukey test, $p < 0.001$; Fig. S5C). No significant differences in mean flow were detected across contingents in 2019, although river flow during this period was significantly higher in 2019 compared to 2020. Food availability measured by chlorophyll-a concentration during the first 30 days of life was significantly affected by contingent (two-way ANOVA, $F_{1,121} = 14.81$, $p < 0.001$), year (two-way ANOVA, $F_{1,121} = 677.41$, $p < 0.001$), and interaction between contingent and year ($F_{3,121} = 8.21$, $p < 0.001$). In 2020, large mesohaline migrants were exposed to significantly higher mean chlorophyll-a concentrations given early hatch dates (Tukey test, $p < 0.01$; Fig. S5D). No differences in mean chlorophyll-a exposure were detected across contingents in 2019, although chlorophyll-a concentrations were significantly higher during this period in 2019 than in 2020.

LITERATURE CITED

Campana SE (2001) Accuracy, precision and quality control in age determination, including a review of the use and abuse of age validation methods. J Fish Biol 59:197–242.

Campana SE, Annand MC, Mcmillan AI (1995) Graphical and statistical methods for determining the consistency of age determinations. Trans Am Fish Soc 124:131–138.

Chang WYB (1982) A statistical method for evaluating the reproducibility of age determination. Can J Fish Aquat Sci 39:1208–1210.

Hoenig JM, Morgan MJ, Brown CA (1995) Analysing differences between two age determination methods by tests of symmetry. Can J Fish Aquat Sci 52:364–368.

Lenth R, Singmann H, Love J, Buerkner P, Herve M (2018) Emmeans: estimated marginal means, aka least-squares means.

Rigby RA, Stasinopoulos DM (2005) Generalized additive models for location, scale and shape. J R Stat Soc Ser C Appl Stat 54:507–554.

SUPPLEMENTARY TABLES

Table S1. Sample size and total length (mean ± SD) of juvenile striped bass used for otolith microstructure and microchemistry analysis collected in each Hudson River sampling location for 2019 and 2020.

	2019		2020	
Region	Total length (mm)	N	Total length (mm)	N
Freshwater	56.7 ± 10.2	19	57.9 ± 8.1	20
Oligohaline	52.4 ± 10.6	20	46.4 ± 6.5	16
Mesohaline	60.0 ± 11.6	21	83.4 ± 14.6	20
Polyhaline	90.3 ± 26.8	9	71.7 ± 15.5	6

Table S2. 10-fold cross-validated classification accuracy (with standard deviations) of the random forest classifier that relied on otolith edge elemental concentrations (Mg, Mn, Sr, Ba) of juvenile striped bass collected at different salinity zones (i.e., freshwater, oligohaline, mesohaline, polyhaline) in the Hudson River and western Long Island Sound. Classification accuracy for each habitat and all habitats combined are shown.

Freshwater	Oligohaline	Mesohaline	Polyhaline	Overall
1.00 (0)	0.85 (0.20)	1.00 (0)	1.00 (0)	0.97 (0.04)

Table S3. Akaike's information criterion (corrected for small sample size; AICc) rankings of the generalized additive mixed model (GAMM) to assess the influence of environmental conditions on the timing of dispersal of juvenile striped bass. ΔAICc shows the differences in Akaike's information criterion (corrected for small sample size) between the best model (rank 1) and a given model. df = degrees of freedom.

Rank	Model	df	AICc	ΔAICc
1	Tidal amplitude + Year	6	36.1	0.00
2	Temperature + Year	6	36.8	0.64
3	Tidal Amplitude + Temperature + Year	8	39.3	3.19
4	Tidal amplitude + Flow + Year	8	45.9	9.76
5	Flow + Year	6	46.5	10.39
6	Flow + Temperature + Year	8	47.2	11.07
7	Tidal Amplitude + Temperature +Flow + Year	10	50.0	13.92

SUPPLEMENTARY FIGURES

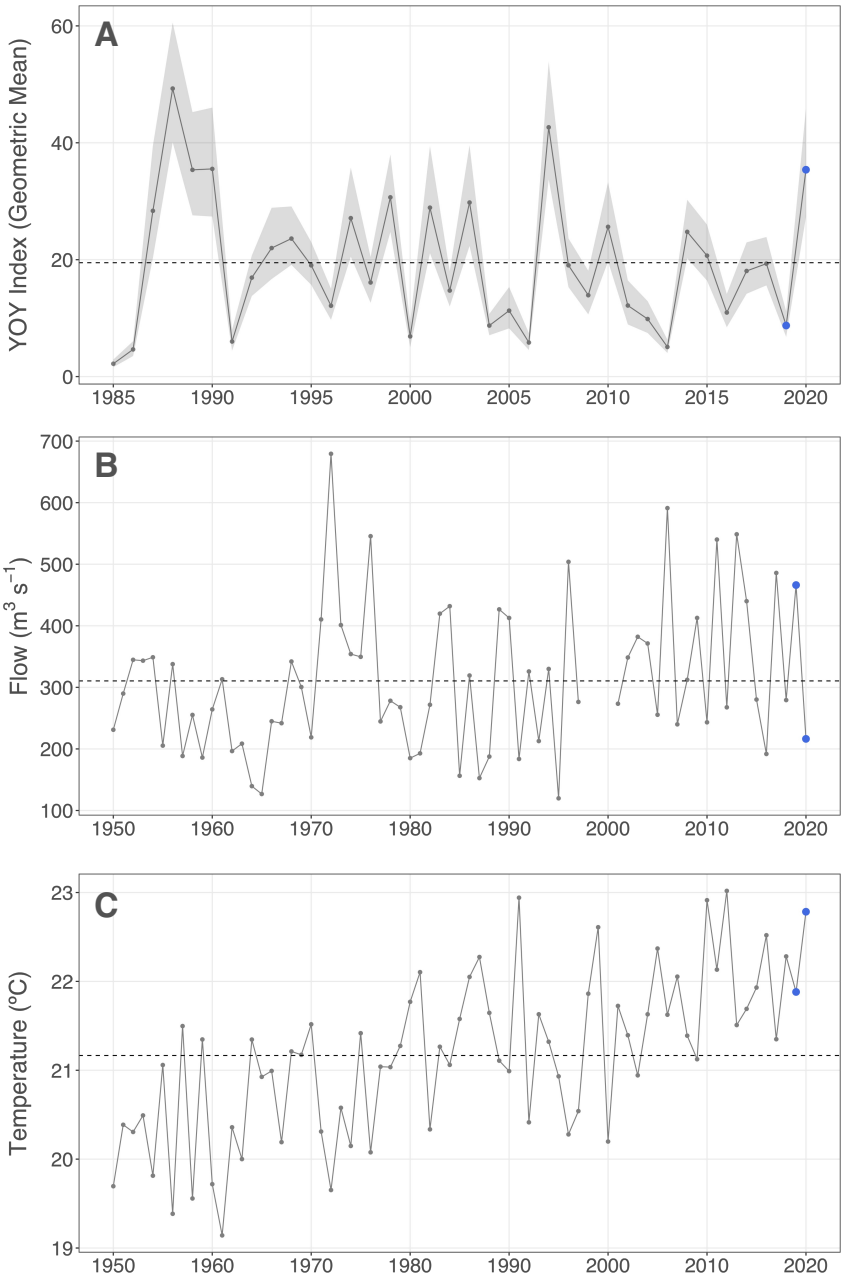

Figure S1. (A) Annual young-of-year striped bass abundance index (1985–2020) estimated from the New York Department of Environmental Conservation (NYDEC) annual young-of-year survey, with shadings indicating 95% confidence intervals. (B) Annual mean (May–August) freshwater flow in the Hudson River (1950–2020), acquired from the USGS Green Island monitoring station (site: 01358000). (C) Annual mean (May–August) water temperature in the Hudson River acquired from the Poughkeepsie Water Treatment Facilities (1950–1991) and USGS monitoring stations (site: 01372058 [1992–2019], 01372043 [2020]) near Poughkeepsie. Blue points for each time series indicate the years of this study (i.e., 2019 and 2020). The horizontal dashed line for each time series indicates the long-term mean for each variable.

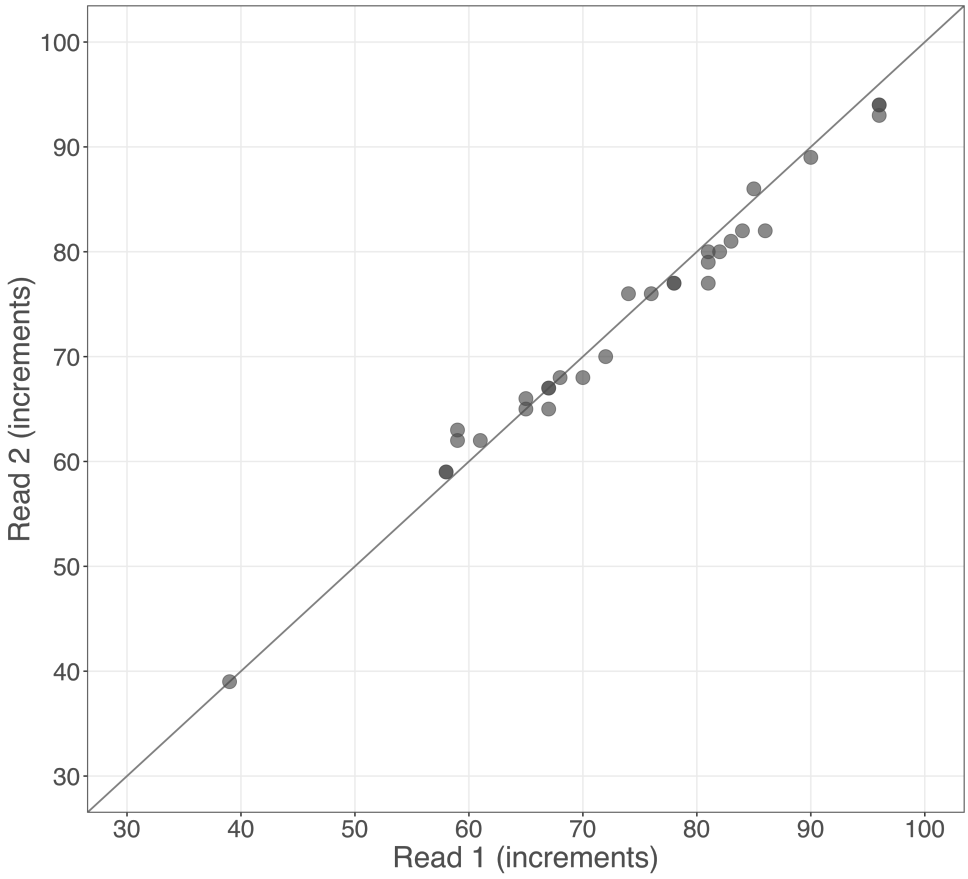

Figure S2. Age-bias plot illustrating matched pairs of Hudson River juvenile striped bass otolith daily increments between two reads. The solid diagonal line indicates the identity line and divergence from the line indicates the degree of systematic differences in matched pairs of increment counts between two reads.

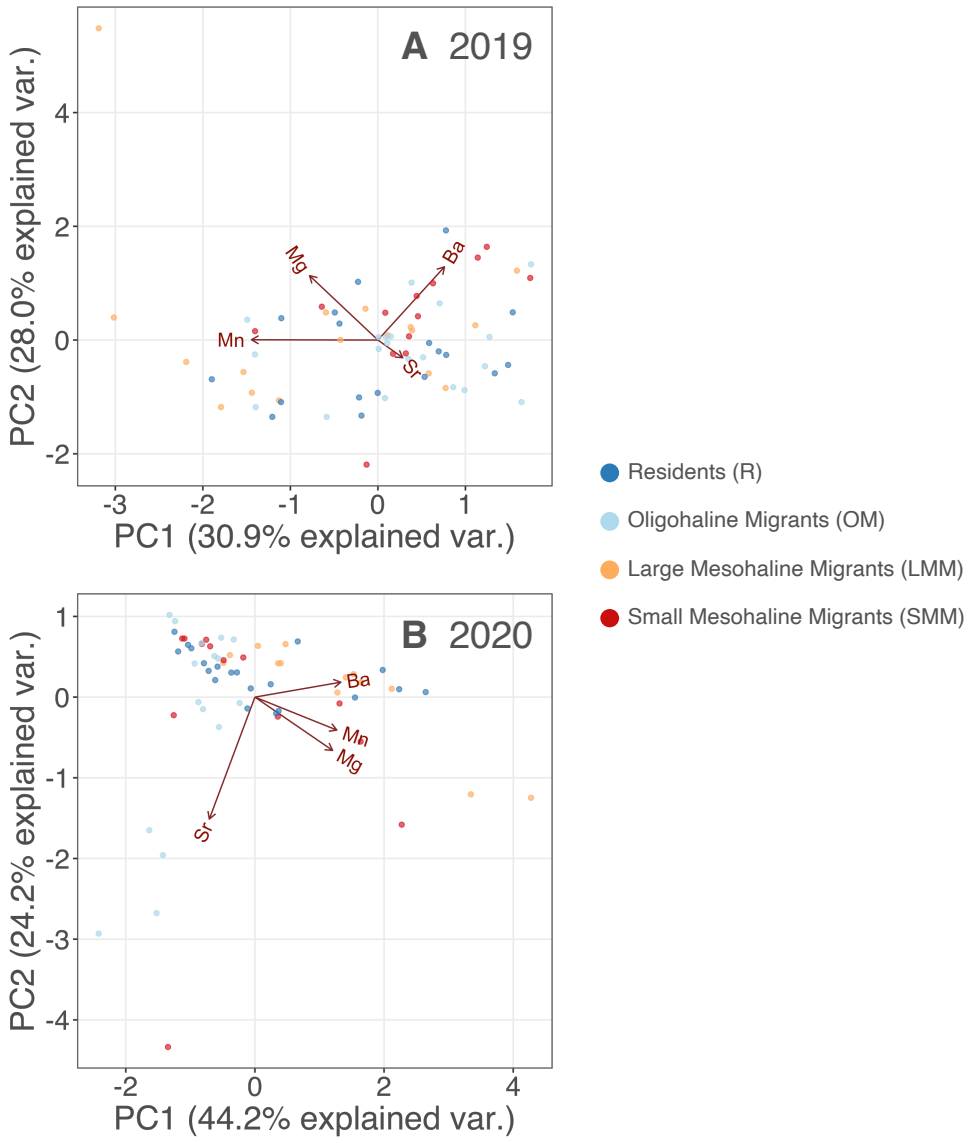

Figure S3. Principal component analysis (PCA) plot depicting mean otolith chemistry (Mg, Mn, Sr, Ba) near the otolith core region of Hudson River juvenile striped bass collected in (A) 2019 and (B) 2020. Different colors indicate assigned migration contingents. Arrows indicate the direction and strength of each variable on the overall distribution. The first two principal components are shown with the variance levels explained on the axes.

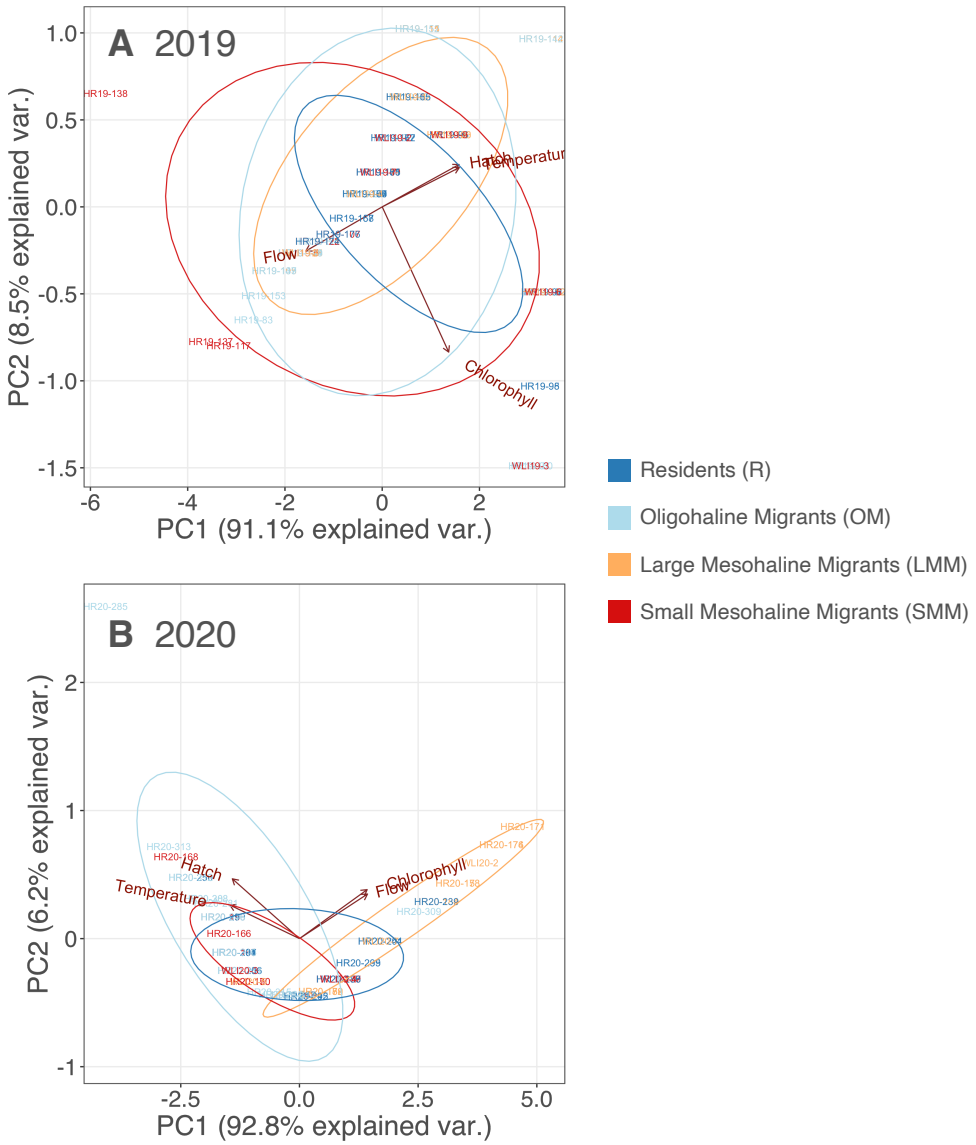

Figure S4. Principal component analysis (PCA) plot depicting the relationship between the hatch date and environmental conditions experienced (mean water temperature, flow, and chlorophyll-a) during the first 30 days of life for individual juvenile striped bass in (A) 2019 and (B) 2020. Each point is labeled by a unique fish ID and different colors indicate assigned migration contingents. Ellipses denote 95% confidence for each migration contingent. Arrows indicate the direction and strength of each variable on the overall distribution. The first two principal components are shown with the variance levels explained on the axes.

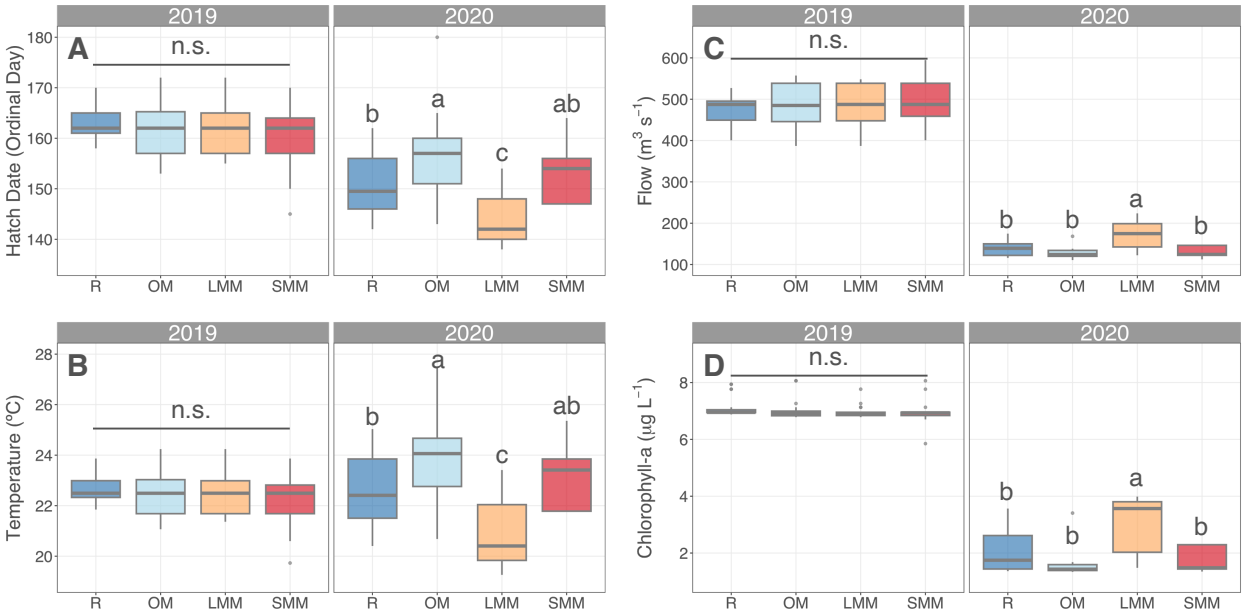

Figure S5. Box whisker plots of (A) hatch dates, and mean (B) water temperature, (C) flow, and (D) chlorophyll-a calculated for the first 30 days of life for resident (R; dark blue), oligohaline migrant (OM; light blue), large mesohaline migrant (LMM; yellow), small mesohaline migrant (SMM; red) juvenile striped bass in 2019 and 2020. Different letters above each box show significant growth differences based on post-hoc Tukey tests ($p < 0.05$). N.S. = no significance detected. The bottom of the box indicates the first quartile ($Q1$), the horizontal line the second quartile ($Q2$ = median), and the top the third quartile ($Q3$). The interquartile range (IQR) is calculated as $Q3 - Q1$, and the whiskers are defined as $Q1 - 1.5 \times IQR$ for the lower whisker and $Q3 + 1.5 \times IQR$ for the upper whisker. Solid circles correspond to observations less than $Q1 - 1.5 \times IQR$ or greater than $Q3 + 1.5 \times IQR$.

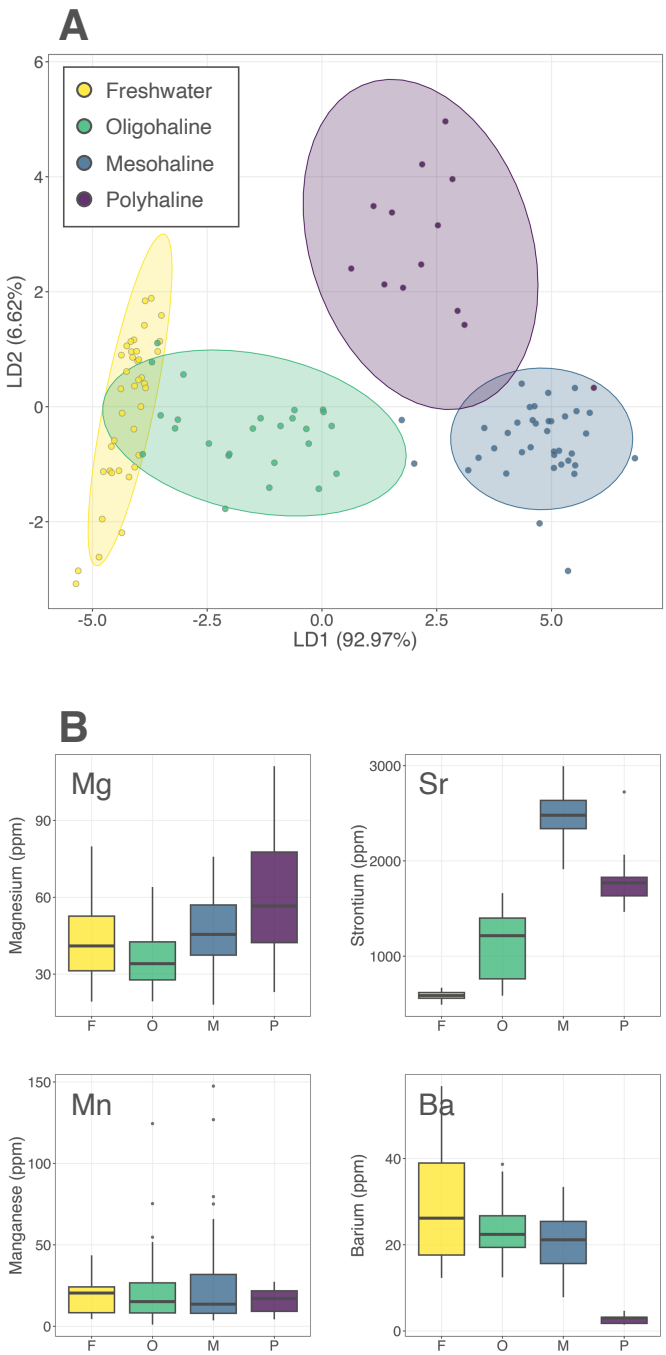

Figure S6. (A) Linear discriminant analysis (LDA) score plot showing the mean edge otolith Mg, Mn, Sr, and Ba for each juvenile striped bass collected in freshwater (salinity < 0.4 ppt), oligohaline (0.4–3.0 ppt), mesohaline (3.0–18.0 ppt), and polyhaline (> 18.0 ppt) habitats used as the reference baseline for random forest habitat assignment. Ellipses show 95% confidence for each habitat. (B) Box whisker plots of mean otolith elemental concentrations (Mg, Mn, Sr, Ba) of the otolith edge for juvenile striped bass collected in different salinity zones in the Hudson River and western Long Island Sound in 2019 and 2020. F = Freshwater, O = Oligohaline, M = Mesohaline, P = Polyhaline.

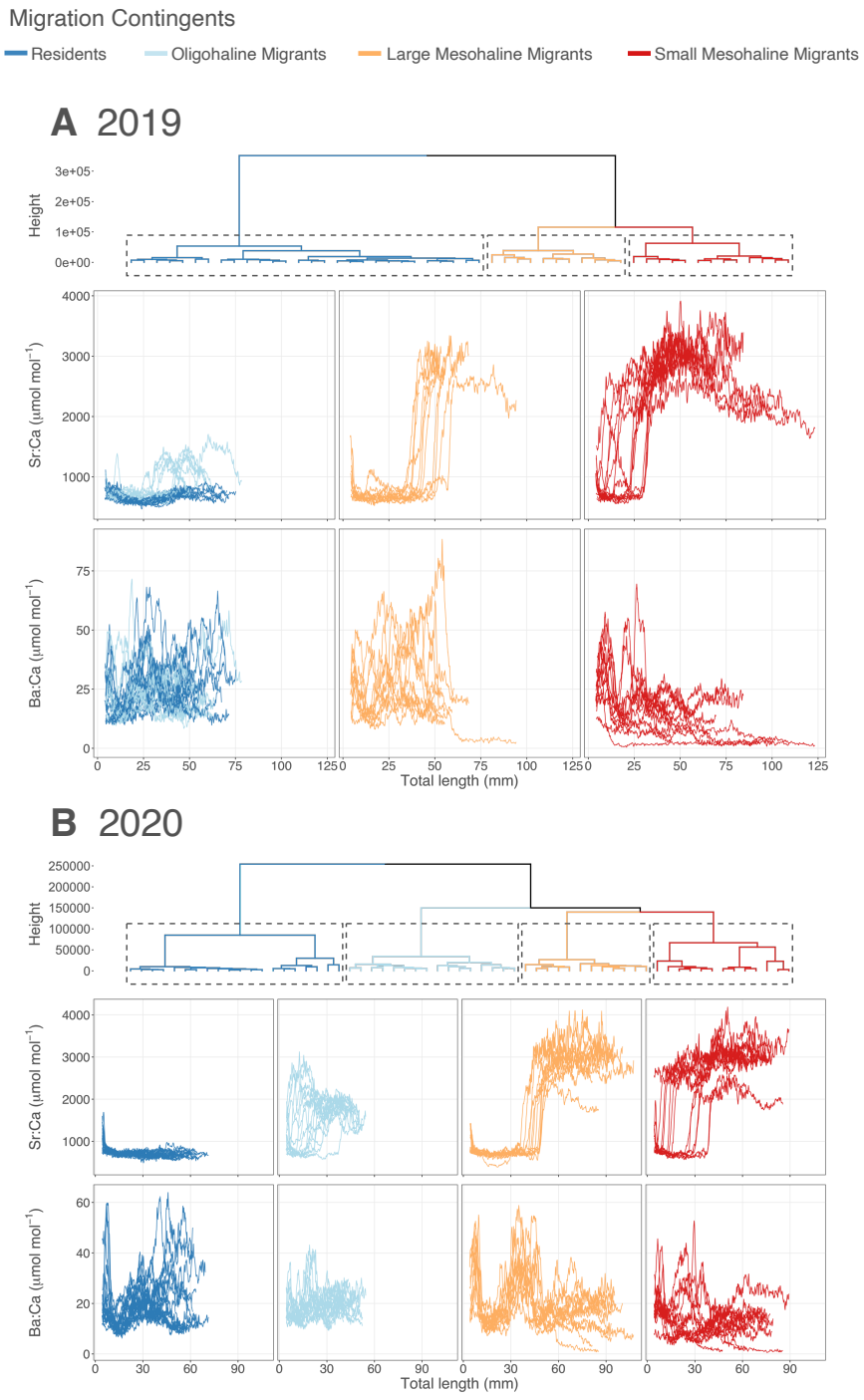

Figure S7. Hierarchical dynamic time warping clustering results using otolith Sr and Ba transects of Hudson River juvenile striped bass for (A) 2019 and (B) 2020. Different colors and dashed rectangles on the dendrogram illustrate distinct clusters (i.e., migration contingents): residents (dark blue), oligohaline migrants (light blue), large mesohaline migrants (yellow), and small mesohaline migrants (red). Note that the y-axis is shown in element:Ca ratios.